Chemical Geology 324-325 (2012) 6–18

Contents lists available at SciVerse ScienceDirect

Chemical Geology

journal homepage: www.elsevier.com/locate/chemgeo

Research paper

Paleoceanographic applications of trace-metal concentration data

Thomas J. Algeo [a],*, Harry Rowe [b]

[a] Department of Geology, University of Cincinnati, Cincinnati, OH 45221-0013, USA
[b] Department of Earth and Environmental Sciences, University of Texas at Arlington, Arlington, TX 76019, USA

ARTICLE INFO

Article history:
Accepted 2 September 2011
Available online 9 September 2011

Editor: J.D. Blum

Keywords:
Molybdenum
Uranium
Vanadium
Zinc
Anoxia
Watermass restriction

ABSTRACT

Recent studies have identified a range of new applications of trace-metal concentration data in the analysis of paleoceanographic systems. In restricted anoxic marine systems, trace-metal/TOC ratios can provide insight into the degree of watermass restriction and estimates of deepwater renewal times. In such systems, secular changes in sediment trace-metal ratios may provide evidence of the chemical evolution of basinal deepwaters in response to differential rates of trace-metal removal to the sediment. The degree of deepwater restriction in silled basins is generally controlled by eustatic elevations, with higher (lower) sea levels resulting in lesser (greater) watermass restriction. Short-term (ca. million-year) drawdown of the trace-metal inventory of seawater has occurred repeatedly in conjunction with oceanic anoxic events, which result in elevated rates of trace-metal removal to widespread anoxic facies. Long-term (eon-scale) changes of the trace-metal composition of seawater have occurred in response to secular changes in atmospheric–oceanic redox conditions and their effects on trace-metal cycling. Caution must be exercised in evaluating trace-metal patterns in paleomarine systems, however: (1) hydrographic analyses based on trace-metal/TOC relationships can be undertaken only on systems that had anoxic deepwaters, and (2) the influence of redox variation on trace-metal accumulation patterns outweighs that of hydrographic factors in some paleomarine systems.

1. Introduction

The application of trace metals to paleoceanographic research has undergone a renaissance as a consequence of recent development of new methods of evaluating trace-metal patterns in marine sediments. Conventionally, trace-metal concentration data were applied mainly to an evaluation of redox conditions in paleomarine systems, with strong enrichment interpreted in terms of reducing environmental conditions (Brumsack, 1980, 2006; Dean et al., 1999; Algeo and Maynard, 2004; Tribovillard et al., 2006). Although redox conditions clearly control differences in trace-metal accumulation rates between oxic (>2.0 ml O_2 L^{-1}), suboxic (2.0–0 ml O_2 L^{-1}), and anoxic facies (Tyson and Pearson, 1991), this relationship does not hold within the anoxic part of the redox spectrum. The transition from weakly sulfidic to strongly sulfidic facies is commonly accompanied by a decline in trace-metal accumulation rates, because hydrographic factors (i.e., limited deepwater renewal) come to dominate over redox influences (Algeo and Lyons, 2006, their Fig. 7). Changes in watermass chemistry associated with hydrographic factors can be recorded by marine sediments, allowing such influences to be recognized in paleomarine systems (Sternbeck et al., 2000; Algeo, 2004; Algeo and Lyons, 2006; Algeo and Maynard, 2008). These insights permit the application of sediment trace-metal concentration data to analysis of a range of chemical and hydrographic properties of paleomarine systems that previously had been unreconstructable (or nearly so): e.g., aqueous concentrations of trace metals, the renewal time of the deep (subpycnoclinal) watermass, and short-term and long-term changes in the trace-metal inventories of seawater. The present contribution is a review of these new applications to paleoceanographic research, with examples drawn both from the literature and from research in progress. This review will focus on molybdenum (Mo) because it is the best-studied trace metal despite uncertainties concerning the vectors of Mo removal to the sediment, specifically whether Mo is hosted by organic or Fe-sulfide phases (Helz et al., 2011). Determination of the degree to which other trace metals mimic the behavior of Mo in response to redox and hydrographic influences will require further investigation.

2. Trace-metal/TOC ratios in modern marine systems

The degree of restriction of the deep (subpycnoclinal) watermass is an important characteristic of marine systems that influences environmental conditions and biogeochemical cycles (Fig. 1). In modern marine systems, the renewal time of the deep watermass can be calculated from aqueous radioisotopic tracers such as ^{14}C and ^{3}H (Top and Clarke, 1983; Östlund and Dyrssen, 1986) or ^{226}Ra and ^{3}He (Falkner et al., 1991; Murray et al., 1991) as well as by several other methods. In paleomarine systems, however, aqueous proxies are not available, and any approach to estimating watermass parameters must rely on a

---

* Corresponding author.
E-mail address: Thomas.Algeo@uc.edu (T.J. Algeo).

0009-2541/$ – see front matter © 2011 Elsevier B.V. All rights reserved.
doi:10.1016/j.chemgeo.2011.09.002

sediment-based proxy. Certain trace metals are suitable for this purpose because they are (1) redox sensitive, thus recording an environmental parameter closely related to watermass restriction, and (2) relatively immobile in the sediment, thus potentially preserving a primary environmental signal.

A method for estimating watermass restriction from sediment trace-metal concentrations was proposed by Algeo and Lyons (2006). The method is based on the observation that the amount of Mo taken up by sediments in anoxic marine systems depends on both the aqueous concentration of Mo (i.e., source-ion availability) and the concentration of sedimentary organic matter (i.e., host-phase availability):

$$[Mo]_s \equiv [TOC]_s \bullet [Mo]_{aq}, \tag{1}$$

$$\text{or}\quad [Mo/TOC]_s \equiv [Mo]_{aq} \tag{2}$$

where TOC is total organic carbon, and the subscripts s and aq denote sediment and aqueous concentrations, respectively. Eq. (2) indicates that the ratio of Mo to TOC in the sediment should be proportional to the concentration of aqueous Mo in the deep watermass. Where $[Mo]_{aq}$ concentrations are high due to relatively unrestricted conditions and strong deepwater renewal, $[Mo/TOC]_s$ ratios will be high. Conversely, where $[Mo]_{aq}$ concentrations are low due to strongly restricted conditions and limited deepwater renewal, $[Mo/TOC]_s$ ratios will be low. Normalization of $[Mo]_s$ to organic carbon is necessary because of the role that organic matter has as a substrate for Mo uptake by the sediment, allowing comparison of levels of sediment Mo enrichment among marine systems containing variable amounts of organic matter.

The validity of these relationships can be demonstrated for modern marine systems (Algeo and Lyons, 2006). Although $[Mo]_{aq}$ concentrations are nearly constant in the global ocean (~105 ± 5 nmol kg^{-1}; Wright and Colling, 1995), they show considerable variation among restricted anoxic marine systems. For example, the $[Mo]_{aq}$ concentration of the deep watermass is ~80–100% of that of open-ocean seawater in Saanich Inlet, 70–85% in Cariaco Basin, 20–30% in Framvaren Fjord, and just 3–5% in the Black Sea (Fig. 2A). In marine systems with higher $[Mo]_{aq}$ concentrations, sediment Mo/TOC ratios are also higher: ~45 in Saanich Inlet, ~25 in Cariaco Basin, ~9 in Framvaren Fjord, and ~4.5 in the Black Sea (Fig. 2B; n.b., all Mo/TOC ratios given in this study represent ppm/% and thus have units of ×10^{-4}). Despite the limited number of modern systems available for analysis, the relationship of $[Mo]_{aq}$ concentrations to $[Mo/TOC]_s$ is robust (Fig. 3A; $r = 0.96$; $p(\alpha) < 0.01$). This relationship exists because, in restricted marine basins with only limited resupply, removal of Mo to the sediment draws down deepwater $[Mo]_{aq}$, thus reducing the rate of removal to the sediment (Fig. 1B–C). The rate of resupply of aqueous Mo by deepwater exchange can be proxied by deepwater renewal times: <10 yr in Saanich Inlet, ~50–100 yr in the Cariaco Basin, ~100–125 yr in Framvaren Fjord, and ~400–800 yr in the Black Sea (Table 1). The importance of deepwater exchange as a control on aqueous [Mo] is demonstrated by the strong negative correlation of the former to the latter parameter (Fig. 3B; $r = 0.92$; $p(\alpha) < 0.01$). Ultimately, deepwater renewal and aqueous [Mo] depend on basin geometry: the subpycnoclinal watermass is renewed less readily in larger basins with shallower sills, such as the Black Sea, than in smaller basins with deeper sills, such as Saanich Inlet (Fig. 1; Algeo and Lyons, 2006).

An important caveat is that this approach to hydrographic analysis is applicable only to paleomarine systems that were anoxic, i.e., in which at least weakly sulfidic conditions (≥10 µmol H_2S L^{-1}) existed in the deep watermass at least part of the time (Algeo and Lyons, 2006, their Fig. 7). Marine systems in which deepwaters were predominantly oxic or suboxic accumulate little authigenic Mo (e.g., Chaillou et al., 2008) because the concentrations of H_2S required to convert molybdate anions (MoO_4^{-2}) to particle-reactive thiomolybdates ($MoO_xS_{4-x}^{-2}$, x = 0

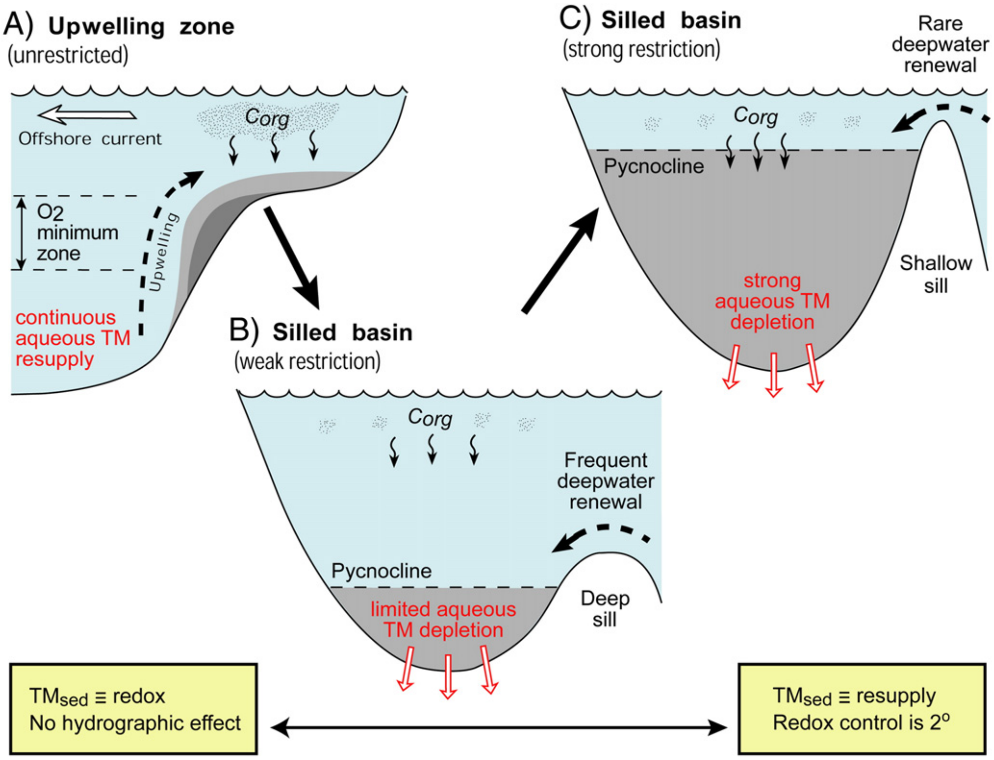

Fig. 1. Models of influences on trace-metal (TM) accumulation in different settings: (A) continental shelf upwelling zone, (B) anoxic basin with deep sill, and (C) anoxic basin with shallow sill. These settings represent a continuum with respect to deepwater restriction. Unrestricted circulation as in A allows continuous resupply of trace metals, resulting in a dominant redox control where trace-metal uptake is proportional to (≡) the intensity of reducing conditions and hydrographic effects are limited. Strongly restricted circulation as in C results in limited resupply of trace metals, favoring a hydrographic control where sediment TM concentrations are proportional to the rate of deepwater renewal and redox effects are secondary.

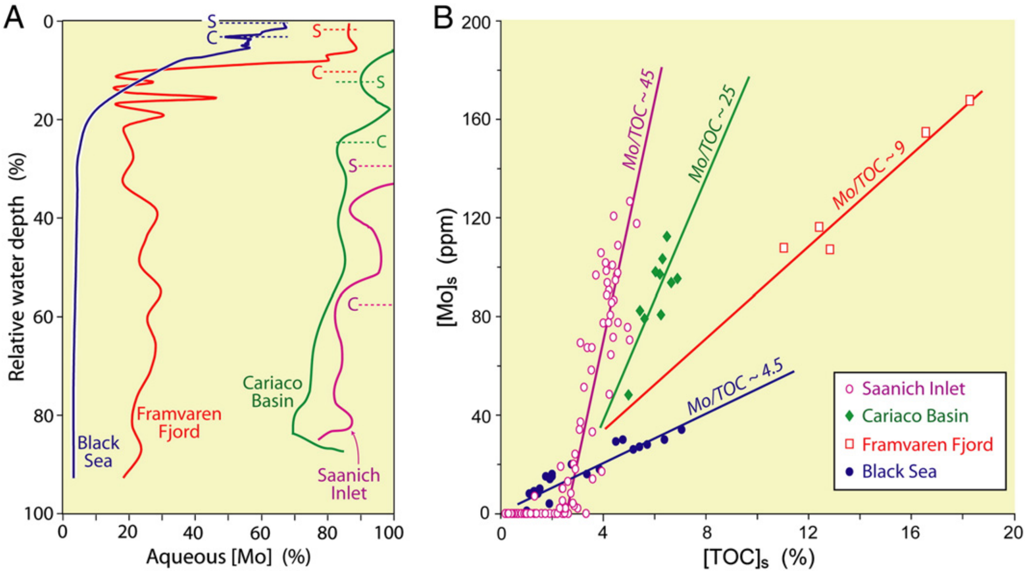

Fig. 2. Modern anoxic silled basins: (A) Aqueous [Mo] versus relative water depth. $[Mo]_{aq}$ is normalized to seawater salinity, i.e., $(Mo/Cl)/(Mo/Cl)_{seawater}$. Relative water depth = water depth/total basin depth. C = chemocline depth, S = basin sill depth. (B) Sediment [Mo] versus [TOC]. Note that all Mo/TOC ratios reported in this study are in units of 10^{-4}, equivalent to ppm/%. Data for surface and near-surface samples only; see Algeo and Lyons (2006) for details.

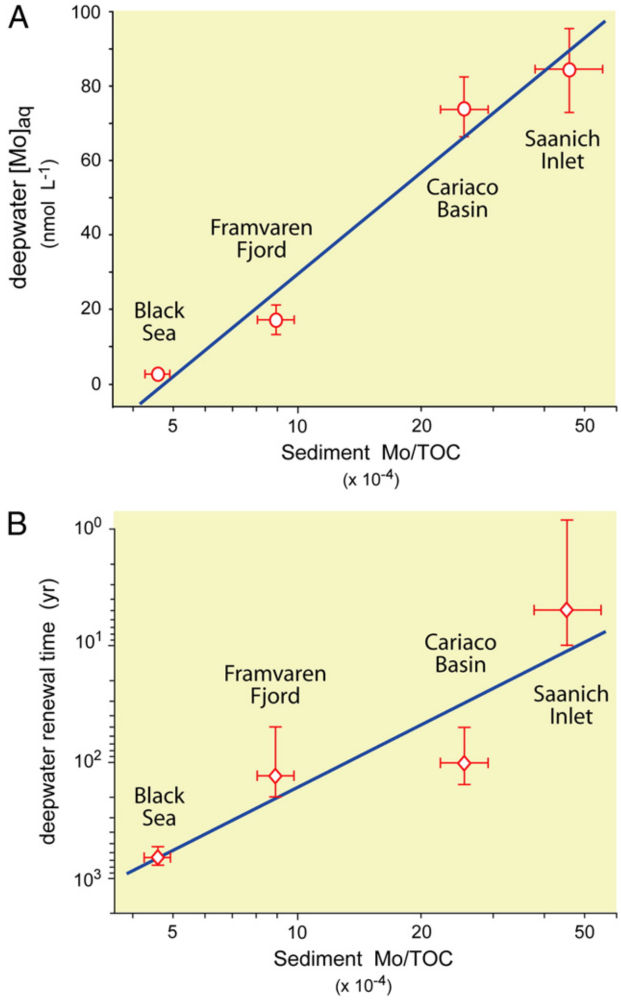

Fig. 3. Modern anoxic silled basins: (A) deepwater $[Mo]_{aq}$ versus $[Mo/TOC]_s$, and (B) deepwater renewal time (τ_{dw}) versus $[Mo/TOC]_s$. Modified from Algeo and Lyons (2006) and using revised τ_{dw} values: Black Sea = 650 ± 125 yr, Framvaren Fjord = 125 ± 75 yr, and Cariaco Basin = 100 ± 50 yr (Table 1). Crosses show estimated uncertainty ranges. Vertical scale in A corrected from figure 8 of Algeo and Lyons (2006).

to 3) are lacking (Helz et al., 1996). In such systems, low $[Mo/TOC]_s$ ratios are a consequence of redox rather than hydrographic controls (e.g., Pattan and Pearce, 2009). This situation is illustrated by modern continent-margin upwelling systems (Fig. 1A), most of which are characterized by persistently suboxic conditions. For example, the SW African Shelf yields $[Mo/TOC]_s$ ratios of ~6 ± 3 (Algeo and Lyons, 2006, their Fig. 5E), the Arabian Sea continental slope yields ratios of ~2–3 (van der Weijden et al., 2006), and the Mexican and Peru shelves yield ratios of ~3–4 and ~10–15, respectively (calculated from data in McManus et al., 2006). All of these values are well below peak $[Mo/TOC]_s$ ratios for restricted anoxic basins (~45–70; Algeo and Lyons, 2006; Algeo et al., 2007) as a consequence of predominantly suboxic rather than restricted

Table 1

Renewal or residence time estimates for the subpycnoclinal watermass of modern anoxic silled basins.[a]

Basin	Level[b]	Age (yr)	Method	Source
Black Sea	Interm.	<100[c]	^{14}C	Östlund and Dyrssen (1986)
Black Sea	Interm.	125–150	^{3}H, ^{3}He	Top and Clarke (1983)
Black Sea	Deep	387–670	T–S modeling	Murray et al. (1991)
Black Sea	Deep	500–600[c]	^{14}C	Östlund and Dyrssen (1986)
Black Sea	Deep	565–600	^{3}H, ^{3}He	Top and Clarke (1983)
Black Sea	Deep	625	CFC modeling	Lee et al. (2002)
Black Sea	Deep	850	^{3}He	Top et al. (1990)
Black Sea	Deep	500–1000	^{226}Ra	Falkner et al. (1991)
Framvaren	Interm.	<15	^{3}H	Dyrssen et al. (1996)
Framvaren	Deep	50–100	^{3}H	Dyrssen et al. (1996)
Framvaren	Deep	123	Si modeling	Yao and Millero (1995)
Framvaren	Deep	1600[d]	^{14}C	Dyrssen et al. (1996)
Cariaco	Deep	70–100	Various	Richards (1975)
Cariaco	Deep	100	^{14}C	Deuser (1973)
Cariaco	Deep	<200	T–S modeling	Scranton et al. (1987)

[a] This table represents a reassessment of renewal/residence time data for modern anoxic marine systems, and the ages reported herein differ somewhat from those given in Algeo and Lyons (2006).

[b] In the Black Sea, the intermediate watermass (~200–400 m) exhibits rapid changes in salinity and potential temperature with depth, whereas the deep watermass (>400 m) exhibits relatively uniform salinity-temperature conditions (Murray et al., 1991). In Framvaren Fjord, the intermediate watermass (18–100 m) is separated by a secondary pycnocline from the deep watermass (100–180 m; Skei, 1983).

[c] C-14 ages reported as 1000–1500 yr (intermediate waters) and 2000 yr (deep waters) by Östlund and Dyrssen (1986) but recalculated by Murray et al. (1991) taking into account dead fossil carbon yielding a ^{14}C age of 1430 yr for surface waters.

[d] C-14 age probably too old owing to dead fossil carbon in surface waters.

euxinic conditions. Further, such systems tend to exhibit strong spatial variability in $[Mo/TOC]_s$ ratios owing to "poikiloxia," i.e., spatially heterogeneous redox conditions.

3. Paleoceanographic applications of trace-metal/TOC ratios

3.1. Hydrographic restriction in paleomarine systems

The relationship of $[Mo/TOC]_s$ to hydrographic properties of modern restricted marine basins (see Section 2) makes feasible hydrographic analysis of paleomarine systems. Algeo and Maynard (2008) showed that it was possible to assess whether a given paleomarine system had a restricted or unrestricted deep watermass on the basis of covariation or lack thereof among trace metals in sedimentary successions. Strong covariation of trace-metal concentrations indicates a dominant redox control on trace-metal accumulation, accompanied by little or no change in the concentration ratios of various trace metals as would be expected in an unrestricted marine system. Carboniferous (Upper Pennsylvanian) cyclothemic shales of midcontinent North America exhibit this pattern of trace-metal covariation (Algeo and Maynard, 2008, their Fig. 7F), implying that Midcontinent Sea deepwaters were in good communication with the Panthalassic (global) ocean to the west (cf. Fig. 1A; Algeo and Heckel, 2008; Algeo et al., 2008a). In contrast, pronounced secular variation in trace-metal ratios in a marine basin may indicate evolution of watermass chemistry in response to differential rates of trace-metal uptake by the sediment. Upper Devonian black shales of the central Appalachian Basin exhibit upsection changes of this type (Algeo and Maynard, 2008, their Fig. 6D), implying that deepwaters of the North American Late Devonian Seaway were isolated within silled intracratonic basins (cf. Fig. 1B–C). For restricted paleomarine systems such as those of the Late Devonian Seaway, aqueous [Mo] and deepwater renewal times can be estimated based on relationships of $[Mo/TOC]_s$ to hydrographic properties of modern restricted marine systems (Fig. 3; Algeo et al., 2007). Subsequently, the $[Mo/TOC]_s$ proxy for watermass restriction has been applied in a series of paleoceanographic studies of Paleozoic and Mesozoic formations (McArthur et al., 2008; Rowe et al., 2008; Hetzel et al., 2009; März et al., 2009; Xu et al., 2009).

An example of extreme watermass restriction may be provided by the Barnett Shale, an organic-rich (to 10% TOC) unit of middle to late Mississippian (Visean to Serpukhovian) age from the Fort Worth Basin of east-central Texas (Loucks and Ruppel, 2007; Rowe et al., 2008, 2009). At that time, the Fort Worth Basin was located on the southern margin of Laurussia, which was a convergent margin in the early stages of the collision with Gondwana that ultimately produced the Ouachita–Marathon Orogeny (Fig. 4A). The basin was encircled by the Laurussian craton to the north, the Llano Uplift to the west, and the Caballos–Arkansas island arc to the south. Because the details of such paleogeographic reconstructions are speculative, the degree of communication of the Forth Worth Basin with the Rheic Ocean to the south or the Panthalassic Ocean to the west is not really known. The Barnett Formation is composed mainly of laminated siliceous and carbonate mudstones deposited at intermediate water depths (~100–200 m) with no evidence of benthic biota above microbial complexity (Loucks and Ruppel, 2007). Redox conditions were generally anoxic–euxinic, as indicated by ubiquitous lamination, high TOC, abundant pyrite, and degree-of-pyritization (DOP) values of 0.50–0.80 (Rowe et al., 2008). Although once inferred to represent normal marine conditions, the Barnett Shale has been reinterpreted as a restricted-marine unit (Loucks and Ruppel, 2007). This hypothesis is consistent with geochemical evidence of extreme watermass restriction: all Barnett facies have low Mo concentrations for a given TOC concentration, yielding a formation average Mo/TOC ratio of ~2 (Fig. 4B; Rowe et al., 2008). In view of the indisputably anoxic–euxinic character of the Barnett paleoenvironment, the most probable explanation for such a low Mo/TOC ratio is a high degree of watermass restriction. Based on comparisons with restricted modern marine systems (e.g., Fig. 3), Rowe et al. (2008) calculated watermass renewal times of ~8 to 20 kyr. These results imply that the Fort Worth Basin was strongly isolated from the Rheic and Panthalassic oceans by the mid- to late Mississippian Period, suggesting the existence of additional tectonic barriers not shown in the paleoceanographic reconstruction of Fig. 4A. More generally, this study shows that trace-metal-based hydrographic analyses have the potential to refine our understanding of geographic and tectonic factors in paleomarine systems.

3.2. Influence of eustatic changes on basinal restriction

The degree of deepwater restriction in a silled marine basin is related to eustatic elevation. Falling eustatic levels generally result in greater restriction owing to reduced water depths over a basin's marginal sills, while rising eustatic levels produce the opposite effect. Exceptions to this pattern are possible, however: if rising eustatic levels are accompanied by warmer, wetter climatic conditions, then outflow of surface waters from a basin may increase to the point that the volume of inflowing deepwater is reduced despite greater water depths over the marginal sills. This situation is inferred to have developed in the Cleveland Basin (Yorkshire, England) during the Toarcian oceanic anoxic event (McArthur et al., 2008, their Fig. 8). Also, eustatic changes can trigger changes in nutrient levels and primary productivity rates that can result in changes in organic carbon fluxes and deepwater redox conditions that are largely independent of the degree of deepwater restriction.

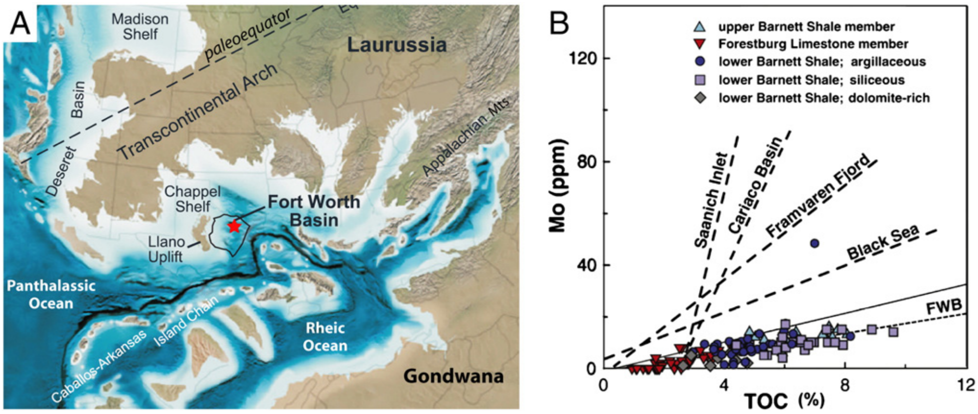

Fig. 4. (A) Early Mississippian paleogeography of southern Laurussia. Modified from Loucks and Ruppel (2007) with base map from Ron Blakey (http://jan.ucc.nau.edu/~rcb7/). Red star shows study site. (B) Barnett Shale $[Mo]_s$–$[TOC]_s$ covariation. Data from Texas United 1 Blakely drillcore, Fort Worth Basin (FWB); modified from Rowe et al. (2008).

For example, rising eustatic levels during the last deglaciation (~16 to 6 kyr B.P.) caused deepening of the sills bounding the modern Cariaco Basin, with a consequent influx of nutrient-rich intermediate waters that stimulated primary productivity and triggered deepwater anoxia (Haug et al., 1998; Yarincik et al., 2000).

The Upper Devonian black shale succession of the central Appalachian Basin provides a case study of the relationship of eustasy to basinal restriction and trace-metal accumulation patterns. During the Late Devonian, this basin was in communication with the Rheic Ocean as well as the adjacent Illinois and Michigan basins across shallow marginal sills (Fig. 5A). Eustatic elevations were mostly rising through the Middle and Late Devonian, a trend representing the 2nd-order Kaskaskian transgression (Fig. 5B; Sloss, 1963; Johnson et al., 1985). However, significant short-term eustatic falls occurred at the Frasnian/Famennian boundary and the Devonian/Carboniferous boundary; the latter event has been linked to a short but severe episode of continental glaciation in South America (Isaacson et al., 2008) that was accompanied by piedmont glaciation in Laurussia (Brezinski et al., 2008). Deepwaters of the Appalachian Basin (and of other cratonic basins) were highly restricted during the initial transgression of the craton, as reflected in Mo/TOC ratios of ~2 in the "Geneseo" Shale, but as sea levels continued to rise during the Frasnian deepwaters became less restricted, yielding Mo/TOC ratios of ~25 in the Upper Olentangy (Fig. 5B; Algeo et al., 2007). The eustatic fall at the Frasnian/Famennian boundary reduced Mo/TOC ratios to ~12–14 in the lower Huron Shale, but these values slowly rebounded to ~16–20 as sea-level rise continued into the late Famennian. The large eustatic fall at the Devonian/Carboniferous boundary commenced during deposition of the upper Cleveland Shale, in which Mo/TOC ratios are reduced to ~7 (Fig. 5B), and culminated in siltstones of the Bedford–Berea lowstand systems tract (Pashin and Ettensohn, 1995; Algeo et al., 2007). The ensuing Early Mississippian transgression produced the widespread Sunbury Shale and yielded Mo/TOC ratios of ~50–60, indicative of relatively unrestricted watermass conditions. Despite large changes in Mo/TOC ratios, redox conditions within the marine environment of the central Appalachian Basin were relatively stable through the Late Devonian, as shown by only limited variation in DOP values (~0.6–0.7; Algeo and Maynard, 2008, their Fig. 6B). Some of the examples of short-term drawdown of trace metals in seawater discussed in Section 3.3 also coincided with eustatic falls, suggesting that similar controls may have operated.

Rates of change in the trace-metal inventories of restricted watermasses in response to eustatic fluctuations can be quite rapid. For example, Mo and other metals in the deep watermass of the modern Black Sea have been drawn down strongly since the marine incursion at ~7540 B.P. triggered by the post-glacial eustatic rise (Jones and Gagnon, 1994). Trace-metal inventories in other restricted marine basins may have been drawn down at even shorter timescales: the most recent deepwater renewal event in the Cariaco Basin was ~100 years ago (Scranton et al., 1987; Holmen and Rooth, 1990; Zhang and Millero, 1993), and the Mo concentration of the deep watermass has declined ~30% since then (Algeo and Lyons, 2006). The time interval required for drawdown of trace-metal inventories in basins having complex histories of watermass chemical changes and linkage to the global ocean (e.g., Framvaren Fjord; Skei, 1983) is more difficult to determine. Replenishment of trace metals to restricted basins, e.g., through seawater incursion as a consequence of eustatic rise, is potentially even more rapid. Replenishment rates via this process would depend principally on the mixing time of the deep watermass, which is typically on the order of decades even for large epicontinental seas (e.g., Algeo et al., 2008b, their Table 1). Such rapid rates of change in seawater composition are generally unresolvable in paleomarine successions and would appear as nearly instantaneous changes in the geologic record.

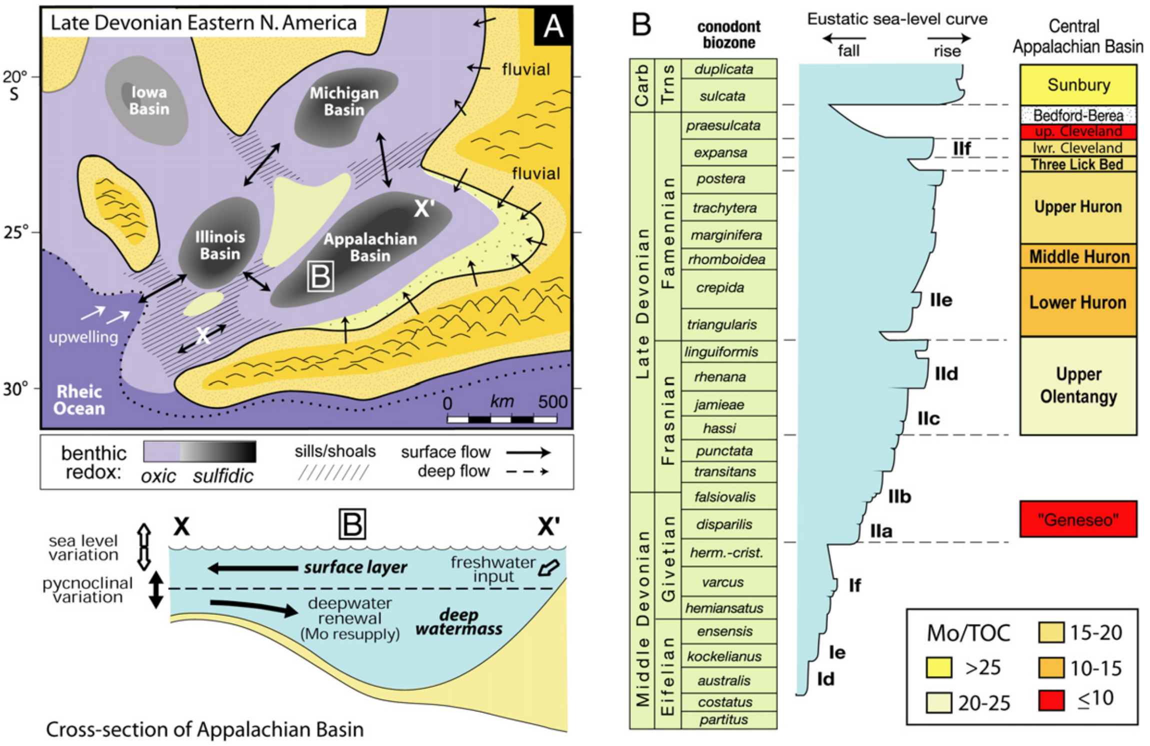

Fig. 5. (A) Paleogeography of eastern North America in the Late Devonian. The cross-section below follows the axis of the Appalachian Basin (X–X′); "B" shows position of stratigraphic column at right. Modified from Algeo and Maynard (2008). (B) Eustatic curve and stratigraphic succession for the Middle Devonian to lowermost Carboniferous of the central Appalachian Basin. Roman numerals indicate transgressive episodes of Johnson et al. (1985); color coding shows average $[Mo/TOC]_s$ ratios for each stratigraphic unit. Modified from Algeo et al. (2007).

3.3. Short-term drawdown of seawater trace-metal inventories

Oceanic anoxic events (OAEs), during which the area of anoxic seafloor expands greatly, can drawdown the trace-metal inventory of seawater through increased rates of trace-metal transfer to the sediment. Such events have the potential to significantly deplete seawater of trace metals—if trace-metal sink fluxes have a first-order relationship to area of anoxic seafloor, then a ten-fold expansion of anoxic seafloor (i.e., from the present 0.3% to just 3%) would induce a ten-fold decrease in trace-metal concentrations in seawater (Algeo, 2004). Most OAEs were geologically short events, often <1 Myr in duration (Jenkyns, 2010), so any reductions in the trace-metal inventory of seawater associated with them were probably of short duration. Following termination of an OAE, trace-metal concentrations in seawater are likely to have rebounded rapidly owing to reduced sink fluxes to diminished areas of anoxic seafloor. The timescale required for such recovery is a function of the residence times (τ_{sw}) of individual trace metals in seawater: ~730 kyr for Mo, ~400 kyr for U, ~50 kyr for V, and shorter for Zn, Cu, Ni, and other metals (Algeo, 2004).

Several examples of episodes of probable trace-metal depletion in seawater during OAEs have now been documented. OAE-2, an anoxic episode of 220 to 800 kyr duration that straddled the ~93-Ma Cenomanian–Turonian boundary, was characterized by enhanced marine productivity and benthic anoxia, especially in the western Tethyan region (Scopelliti et al., 2006; Turgeon and Brumsack, 2006). In a study of organic-rich sediments from the Demerara Rise in the central Atlantic Ocean, Hetzel et al. (2009) demonstrated that, despite concurrent increases in TOC (Fig. 6A) and shifts in redox proxies (Fe_T/Al) toward more reducing conditions (Fig. 6B), the concentrations of various trace metals (including Mo, V, and Zn) declined during this event (Fig. 6C–E). On a TOC-normalized basis, $[Mo/TOC]_s$ decreased from ~8–11 to ~2–3 during OAE-2 before recovering to ratios of ~5–10 following the event (Fig. 6F). $[V/TOC]_s$ and $[Zn/TOC]_s$ show similar patterns of stratigraphic variation through the event interval (Hetzel et al., 2009, their Fig. 11). The most likely explanation of these patterns is that Mo and other trace metals were substantially depleted in seawater, possibly at a global scale but more likely at a regional scale within the juvenile Atlantic Ocean basin. Hetzel et al.'s study site was located in a deep (>1000 m) and probably restricted marine basin, having watermass exchange primarily with surface and intermediate waters of the western Tethys Ocean.

Another example of probable trace-metal depletion in seawater occurred during the ~183-Ma Toarcian OAE of the Early Jurassic. This anoxic event, which lasted between 200 and 900 kyr (McArthur et al., 2008; Suan et al., 2008), is documented by negative C-isotope excursions and other proxies indicative of changes in global seawater composition (Cohen et al., 2004; Pearce et al., 2008; Suan et al., 2008). Organic-rich shales were deposited in a semi-restricted basin of regional extent, encompassing parts of the United Kingdom, France, and Germany, and surrounded by shallow shelf seas extending across the West European platform. McArthur et al. (2008) showed that the degree of watermass restriction varied across the platform, being strongest in areas that were deeper and more distant from the Tethys Ocean, such as the Cleveland Basin (Yorkshire, England). There, upper Pliensbachian–lower Toarcian shales yielded $[Mo/TOC]_s$ ratios of <2 in the upper *semicelatum* and *exaratum* Subzones, providing evidence of extreme watermass restriction, whereas the overlying *falciferum* Subzone yielded ratios of ~5–12, indicative of somewhat improved deepwater ventilation as a consequence of rising eustatic elevations (Fig. 7; McArthur et al., 2008). Based on an analysis of Mo-isotope variation, Pearce et al. (2008) hypothesized that enhanced transfer of Mo to the sediment during the Toarcian OAE resulted in depletion of Mo in contemporaneous seawater.

Episodes of expanded marine anoxia during the Late Devonian also may have resulted in short-term drawdown of trace metals in seawater. Drawdown may have occurred during the latest Devonian Hangenberg Event, corresponding in North America to the upper Cleveland Member of the Ohio Shale and its lateral equivalents (Fig. 5B; Algeo, 2004; Algeo and Maynard, 2008). A second episode of drawdown may have occurred at the Frasnian/Famennian boundary, as recorded in a succession of alternating organic-rich and organic-poor shales in the Hanover and Dunkirk formations in the West Valley core of western New York State (Fig. 8). The organic-poor layers contain low concentrations of TOC and Mo and represent oxic–suboxic facies; they should be disregarded in looking at chemostratigraphic trends. The organic-rich layers contain >2% TOC and represent anoxic facies. They exhibit distinct stratigraphic patterns, with maximum values of TOC and minimum values of Mo, Mo/TOC, U/TOC, and Re/TOC around the Frasnian/Famennian boundary (Fig. 8B–E). These patterns were not controlled by redox changes, since the organic-rich layers exhibit relatively invariant DOP values (~0.6 ± 0.1; Fig. 8A). The Frasnian/Famennian boundary appears to have been associated with a short-term eustatic fall (Playford et al., 1989; Algeo et al., 2007), and, thus, the pattern of lower trace-metal concentrations can be attributed to increased basin restriction and drawdown of trace-metal inventories within Appalachian Basin deepwaters. The durations of these drawdown events can be estimated from cyclostratigraphic analysis: the Cleveland Shale episode represents ~400–500 kyr, while the Frasnian/-Famennian boundary episode represents ~200 kyr (T.J. Algeo and L. Hinnov, unpubl. data).

Demonstrating that changes in trace-metal/TOC ratios in ancient anoxic facies are a product of changes in the aqueous concentration of trace metals is inherently difficult. However, all of the examples cited above pass one important test: the chemostratigraphic profiles exhibit short-term stability and gradual changes in trace-metal/TOC ratios, as might be expected in a basin with slowly evolving watermass chemistry. In contrast, where rapid stratigraphic shifts in trace-metal/TOC ratios occur, such patterns are likely to be controlled by abrupt changes in environmental (e.g., redox) conditions or major changes in lithology (e.g., Three Lick Bed, Algeo and Maynard, 2008, their Fig. 6D). Evaluating controls on trace-metal/TOC patterns requires additional lithologic and environmental proxy data as well as cautious interpretation of the data by investigators.

The areal extent of trace-metal depletion of seawater during OAEs is generally difficult to determine. Trace-metal depletion may (1) affect seawater globally, (2) be limited to the watermass of the depositional basin of interest, or (3) occur at both scales but with a relatively larger drawdown regionally and a smaller drawdown globally. Because observations come mainly from epicratonic seas that are often restricted, it is difficult to "get a read" on changes in the composition of global seawater. However, if observations are available from multiple, hydrographically independent basins of the same age, it may be possible to draw relevant inferences. Where such basins show a wide range of $[Mo/TOC]_s$ ratios (as in cratonic North American basins of Devonian–Carboniferous age; Algeo et al., 2007), it can be inferred that the differences are mainly due to interbasinal variation in the degree of deepwater restriction and consequent effects on local seawater chemistry (cf. Algeo and Maynard, 2008). However, basinal processes, if sufficiently widespread, vigorous, and sustained, have the potential to alter trace-metal inventories in global seawater. Recognizing the signature of a change in global seawater chemistry based on sediment trace-metal concentrations is likely to be difficult, though not impossible. One line of evidence for such an event might be parallel, concurrent changes in $[metal/TOC]_s$ ratios in multiple, hydrographically independent basins, although such a multi-basinal pattern has not been documented to date. Another promising approach to evaluation of global-scale changes in marine redox conditions is the use of Mo isotopes (Anbar and Rouxel, 2007; Pearce et al., 2008; Herrmann et al., this volume) and U isotopes (Weyer et al., 2008; Montoya-Pino et al., 2010; Brennecka et al., in press). These trace metals have the potential to reflect global changes in

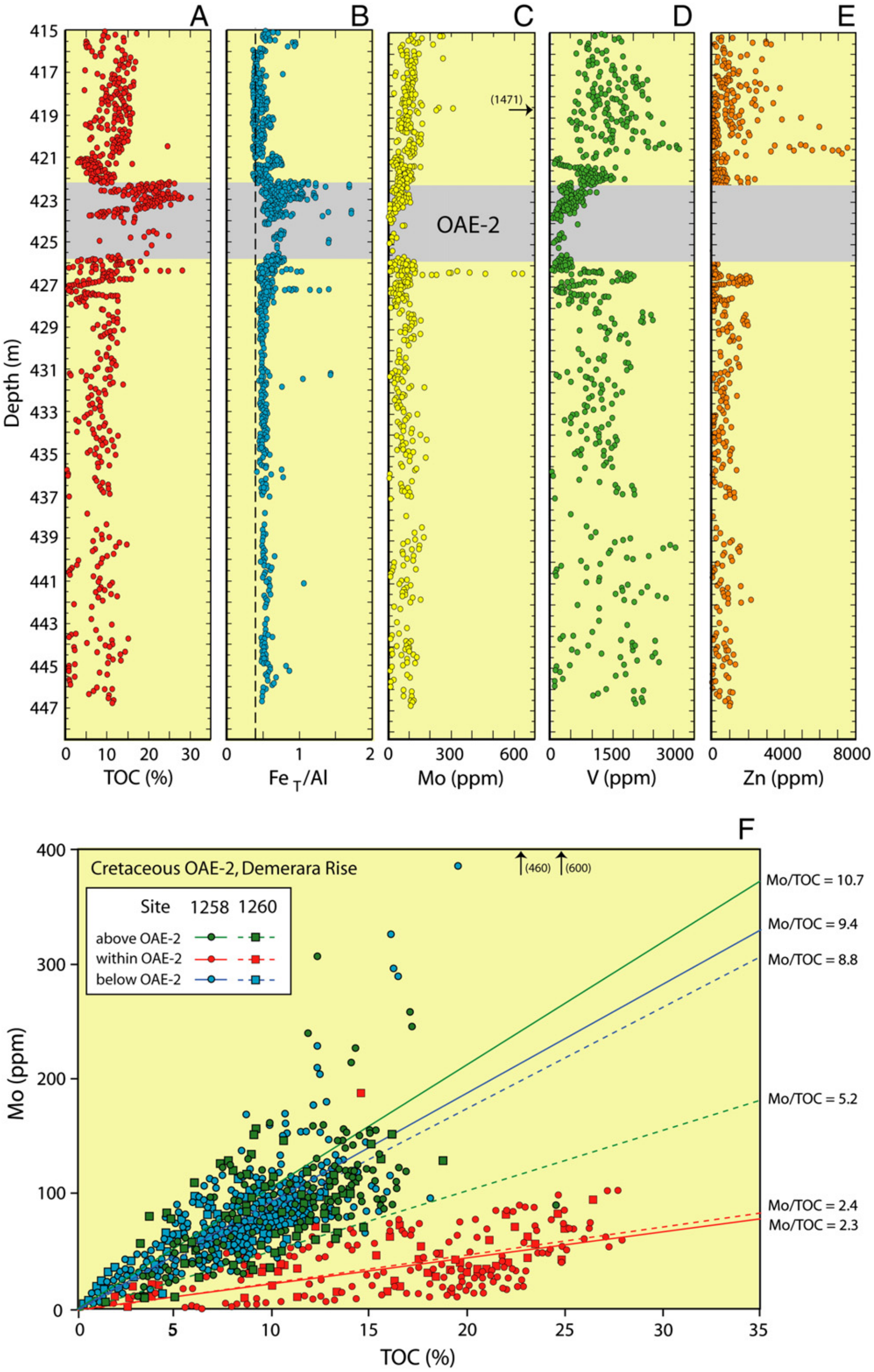

Fig. 6. Middle Cretaceous OAE-2 shales (Cenomanian–Turonian), Demerara Rise, ODP Site 1258. (A) TOC, (B) Fe_T/Al, (C) Mo, (D) V, and (E) Zn. (F) TOC vs. Mo. Modified from Hetzel et al. (2009).

seawater redox conditions and trace-metal inventories owing to residence times in seawater that far exceed the oceanic mixing time of ~1–2 kyr (Wright and Colling, 1995).

3.4. Long-term evolution of global seawater chemistry

The chemical composition of seawater almost certainly has evolved through the course of Earth history. Changes in the major ion composition of seawater have been proposed on the basis of secular variation in the chemistry of evaporite mineral deposits and sedimentary fluid inclusions (Holland, 1984; Hardie, 1996; Lowenstein et al., 2003). Changes in the isotopic composition of major (e.g., DIC, SO_4^{-2}) and minor (e.g., Sr, Os) components of seawater through time are well documented (Strauss, 1999; Veizer et al., 1999; Pegram and Turekian, 1999; McArthur et al., 2001). The total concentration of dissolved species (i.e., salinity) of seawater has probably changed also, among other reasons

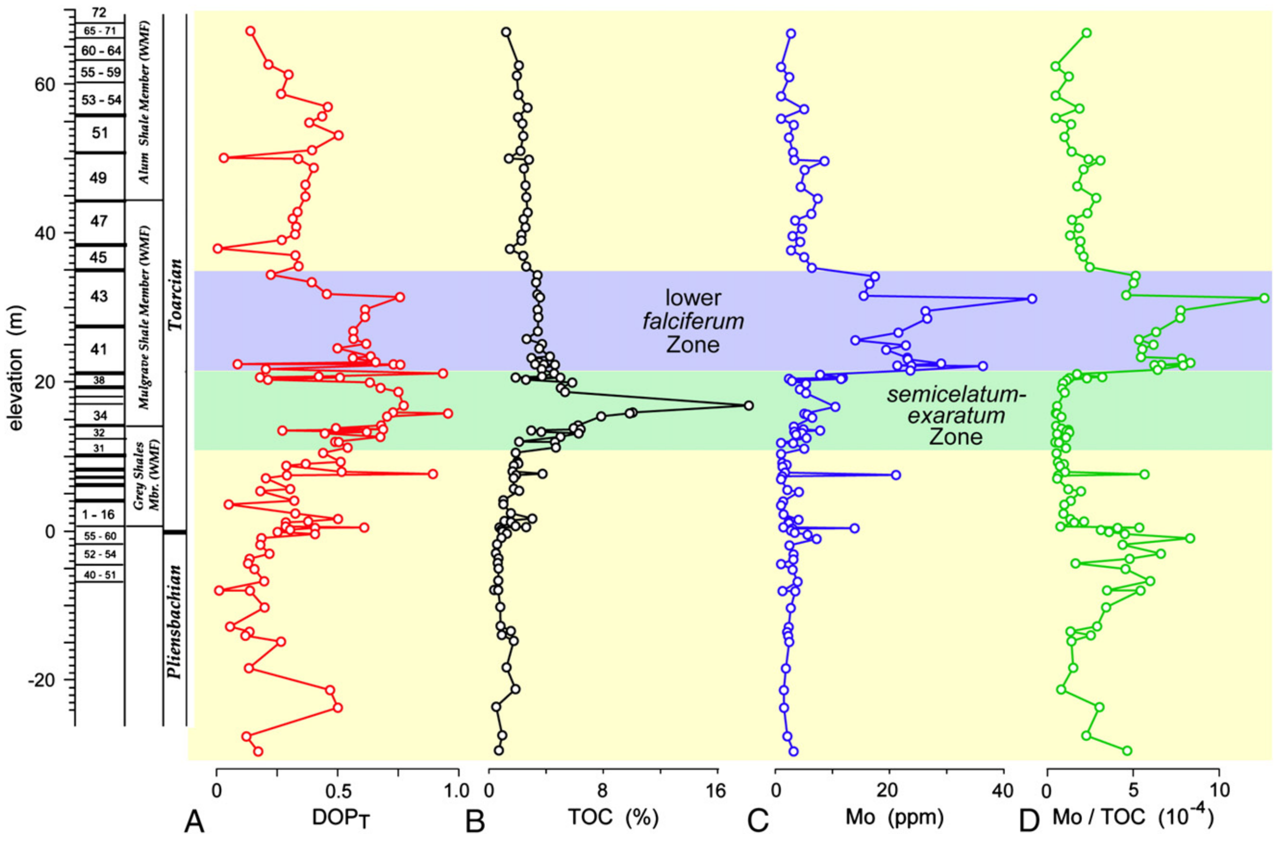

Fig. 7. Lower Jurassic Toarcian–OAE shales, Cleveland Basin (Yorkshire, England). (A) DOP$_T$, (B) TOC, (C) Mo, and (D) Mo/TOC. Colored bands identify the main anoxic intervals discussed in the text. DOP$_T$ is an estimate of DOP (degree of pyritization) based on total Fe rather than highly reactive Fe. Modified from McArthur et al. (2008).

owing to the highly episodic removal of salt through massive evaporite precipitation (Hay et al., 2006). More uncertain, however, are secular changes in the trace-metal inventory of seawater. Understanding such variation is important, however, because certain trace metals play essential roles in biogeochemical processes, e.g., Mo and/or V in nitrogenase, an enzyme used by nitrogen-fixing bacteria, and Cu and Zn in many other enzymes and proteins (Kieffer, 1991; Anbar, 2004; Glass et al., 2009). A paleocean containing significantly lower concentrations of these trace metals might have seriously perturbed biogeochemical cycles (Anbar and Knoll, 2002).

The trace-metal inventories of global seawater may have varied only to a limited degree during the Phanerozoic. Although some short-term variation occurred in conjunction with OAEs (see Section 3.3), it is possible that these effects were largely confined to individual basins and that global seawater experienced rather limited changes in trace-metal inventories. One key observation suggests that the concentration of Mo in seawater has probably not varied greatly during the Phanerozoic (542 Ma to present): the distributions of $[Mo/TOC]_s$ ratios for modern and ancient restricted marine facies are nearly the same. For example, Algeo et al. (2007) reported that Devonian–Carboniferous shales yield $[Mo/TOC]_s$ ratios between 2 and 65 (n = 50; mean ~20), and Scott et al. (2008) reported that more than 90% of organic-rich facies of Phanerozoic age yield $[Mo/TOC]_s$ ratios between ~5 and 45 (n = ~100; Fig. 9)—both distributions being similar to that for modern anoxic marine facies (4.5–45; n = 4; Fig. 2B). If the $[Mo/TOC]_s$ ratio of each formation is viewed as a random sample of the values that might be produced under the range of oceanographic conditions existing in a given geologic period, then the similar distributions of values for ancient and modern anoxic marine facies imply relatively uniform concentrations of Mo in seawater throughout the Phanerozoic.

Long-term (>1-Myr) changes in the concentrations of trace metals in seawater would require sustained changes in trace-metal source or sink fluxes. Changes of this type are likely to have occurred only under atmospheric–oceanic redox conditions radically different from those at present. Such conditions existed during the Precambrian, when the partial pressure of atmospheric O_2 was <10% of its present value (Canfield, 1998; Anbar and Knoll, 2002; Lyons et al., 2009). Archean anoxic marine facies yield $[Mo/TOC]_s$ ratios that are uniformly <3, whereas those of Proterozoic age average ~6 and range up to 25 (Fig. 9; Scott et al., 2008; Lyons et al., 2009). Very low Mo concentrations and Mo/TOC ratios for Archean sediments reflect an absence of oxidative subaerial weathering and consequent limited delivery of Mo to the ocean (Anbar et al., 2007; Kendall et al., 2010). Oxidative weathering increased strongly following the 'Great Oxidation Event' at 2.45–2.32 Ga (Bekker et al., 2004). The $[Mo/TOC]_s$ values of anoxic marine facies varied somewhat systematically through the Proterozoic, exhibiting a mode of ~10–15 from 2.3 to 1.7 Ga, declining to values uniformly <5 from 1.7 to 0.7(?) Ga, and then rising again to ~10–15 from 0.7(?) to 0.54 Ga (Fig. 9; Scott et al., 2008). This pattern has been attributed not to fluctuations in atmospheric pO_2 but, rather, to a sulfidic deep ocean during the Middle and early Late Proterozoic (Canfield, 1998). Sulfidic deepwaters would have enhanced removal of Mo to the sediment, keeping seawater Mo concentrations low and the residence time of Mo in seawater short (Scott et al., 2008; Kendall et al., 2009, 2010). The largest and most abrupt shift in $[Mo/TOC]_s$ occurred in the late Neoproterozoic, when values increased rapidly to the modern range. This event was likely the consequence of a rapid rise in atmospheric pO_2 (Canfield, 2005; Lyons et al., 2009), possibly due to enhanced burial of organic carbon by newly evolved metazoans (Logan et al., 1995). The Neoproterozoic/Phanerozoic boundary at 542 Ma is also

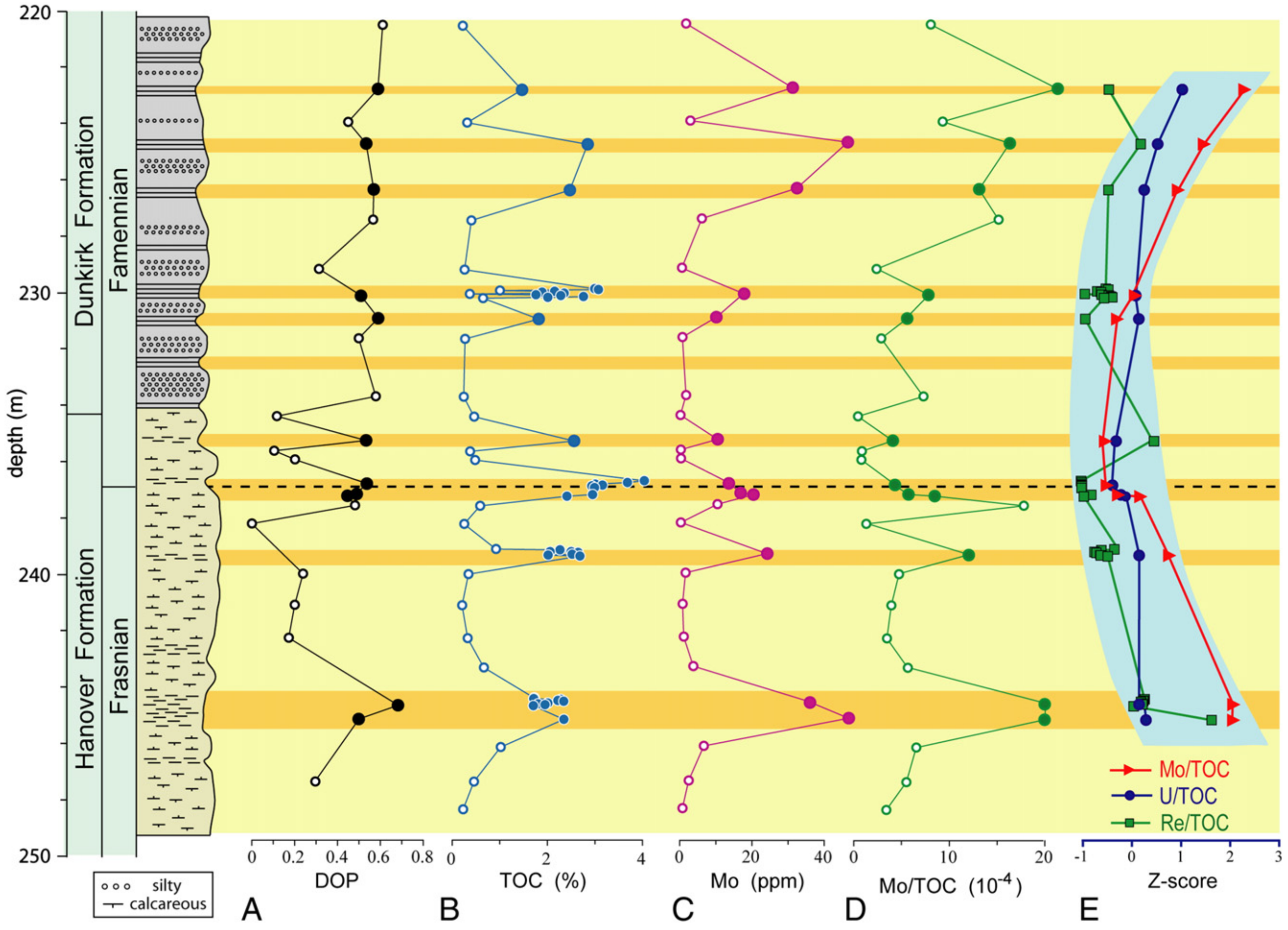

Fig. 8. Upper Devonian Frasnian–Famennian boundary. (A) DOP, (B) TOC, (C) Mo, (D) Mo/TOC, and (E) Z scores for trace-metal/TOC ratios. Samples representing the organic-rich layers discussed in the text (horizontal orange bands) are shown by larger solid symbols; samples representing organic-lean layers are shown by smaller open symbols. In E, results are shown only for the organic-rich layers. Z scores represent values normalized to a mean of zero and a standard deviation of one; the purpose is to compare profiles of trace metals with widely differing raw concentrations. The blue field highlights secular variation in Z scores, including a pronounced minimum around the F/F boundary. Data from West Valley core, western New York State (Algeo et al., in prep.).

characterized by a large shift in Mo isotope ratios, from about +2.0 to 0‰ (δ^{98}Mo), which may be an indication of a rapid (<100 kyr) mixing of a previously stratified ocean with a sulfidic deep watermass (Wille et al., 2008), an event that has implications for macroevolutionary patterns and the “Cambrian Explosion.”

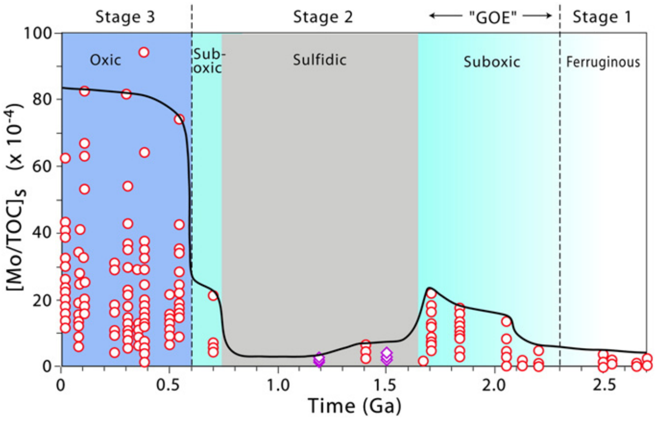

Fig. 9. Temporal trends in Mo/TOC ratios of anoxic facies since 2.7 Ga. Red circles are euxinic shales; purple diamonds are non-euxinic, organic-rich shales. GOE is the ‘Great Oxidation Event.’ Modified from Scott et al. (2008). Stages refer to Earth-surface oxidation history and redox designations indicate deep-ocean conditions; adapted from Canfield (1998) and Lyons et al. (2009).

4. Conjoint hydrographic and redox controls on trace-metal accumulation

The roles of redox versus hydrographic influences on trace-metal accumulation in a marine system can be investigated through crossplots of [Mo/TOC]$_s$ versus DOP (degree-of-pyritization), a common redox proxy (Raiswell et al., 1988), [Mo/TOC]$_s$ is potentially subject to both redox and hydrographic influences, and its relationship to DOP can assist in identifying the relative importance of these factors. Such relationships can be examined either in a spatial context, which is straightforward for modern marine systems sampled at multiple sites, or in a temporal context, which is the de facto mode for paleomarine systems sampled in a vertical stratigraphic section. Uniform [Mo/TOC]$_s$ values within a marine system that shows spatial or temporal variation in redox conditions are evidence for control of trace-metal accumulation by hydrographic factors, and stratigraphic variation in [Mo/TOC]$_s$ independent of DOP is evidence for secular changes in aqueous Mo concentrations. On the other hand, covariation between [Mo/TOC]$_s$ and DOP is evidence for either a direct or indirect redox control of trace-metal accumulation. A direct redox control results in increasing [Mo/TOC]$_s$ with more reducing conditions (Zheng et al., 2000), but such an effect generally should be manifested only in the oxic to weakly sulfidic part of the redox spectrum; under more reducing conditions, hydrographic controls tend to become dominant (Algeo and Lyons, 2006). Indirect redox influence on trace-metal accumulation can result when redox conditions covary with another environmental factor (e.g., watermass restriction or salinity) that is the main control on the rate of authigenic uptake of trace metals by the sediment (see example of Toarcian shales below). These concepts can be illustrated by examination of relationships in several modern and ancient marine systems.

In modern anoxic marine basins in which hydrographic influences are dominant, a limited range of $[Mo/TOC]_s$ ratios are encountered regardless of variation (or lack thereof) in DOP values. This pattern characterizes the abyssal Black Sea (1900–2200 m water depth), where all stations yield $[Mo/TOC]_s$ ratios of 4–7 despite variation in DOP values from 0.35 to 0.8 (Fig. 10A). Shallower stations (<250 m water depth) yield $[Mo/TOC]_s$ ratios close to zero owing to frequent exposure to oxic conditions associated with turbidite flows (Östlund and Dyrssen, 1986; Lyons, 1991). The Cariaco Basin exhibits more uniform DOP values (mostly 0.5–0.6), indicating only limited redox fluctuations in the deep watermass over the last ~15 kyr (Fig. 10B). $[Mo/TOC]_s$ ratios exhibit wider variation than in the Black Sea although this is likely to have resulted from changes in deepwater $[Mo]_{aq}$ through time: low ratios (<10) prior to 14.9 kyr reflect primarily oxic–suboxic conditions, high ratios (30–65) at 14.9–11.5 kyr record the shift to anoxic conditions accompanied by initially high $[Mo]_{aq}$, and intermediate ratios (15–30) since 11.5 kyr represent anoxic sedimentation at somewhat depleted $[Mo]_{aq}$ (Algeo and Lyons, 2006, their Fig. 9). In contrast, Saanich Inlet shows significant positive covariation between DOP_T (over the range 0.2–0.5) and $[Mo/TOC]_s$ (Fig. 10C). This relationship reflects the influence of predominantly oxic–suboxic conditions on samples with DOP values closer to 0.2, and of predominantly anoxic conditions on samples with DOP values closer to 0.5. These sediments are moderately organic-rich (TOC = 0.4–5.3%; mean 2.3%) and are known to have been deposited under redox conditions that fluctuated from oxic to mildly sulfidic (Algeo and Lyons, 2006).

The relationship of $[Mo/TOC]_s$ to DOP in paleomarine systems can be interpreted based on the principles and examples given above. Upper Devonian shales of the central Appalachian Basin collectively exhibit substantial variation in both DOP and $[Mo/TOC]_s$ (Fig. 11A), but all units except the Sunbury Shale show a narrow range of $[Mo/TOC]_s$ ratios that is formation-specific: ~3–4 for the "Geneseo" Shale, ~10–20 for the Huron Shale, ~15–20 for the Three Lick Bed, ~18–25 for the lower Cleveland Shale, and ~3–10 for the upper Cleveland Shale. $[Mo/TOC]_s$ ratios for individual units show no relationship to redox conditions as proxied by DOP, and the range of DOP values is similar for most units (~0.5–0.8) despite large differences in $[Mo/TOC]_s$ ratios. Based on these observations, the differences in $[Mo/TOC]_s$ ratios among the units can be interpreted to reflect variation in deepwater $[Mo]_{aq}$ and, hence, the dominance of hydrographic controls on trace-metal accumulation. The Sunbury Shale differs in exhibiting a wide range of $[Mo/TOC]_s$ ratios (~10–40) despite fairly uniform DOP values (mostly 0.70–0.85; Fig. 11A). A marginally significant positive relationship between DOP and $[Mo/TOC]_s$ ($r^2 = 0.12$) may indicate weak influence by redox conditions on trace-metal accumulation, although it is perhaps more likely that variation in $[Mo/TOC]_s$ represents secular changes in deepwater $[Mo]_{aq}$, similar to those that occurred in the Cariaco Basin over the past 15 kyr (Fig. 10B).

Covariant relationships between $[Mo/TOC]_s$ and DOP are suggestive of redox control of trace-metal accumulation, as seen in some paleomarine units. One example is the Toarcian shales of the Cleveland Basin (Yorkshire, England; Fig. 11B). Whereas shales of the *semicelatum–exaratum* Zones exhibit uniformly low $[Mo/TOC]_s$ ratios (<3), indicative of extreme watermass restriction, shales of the overlying *falciferum* Zone exhibit higher $[Mo/TOC]_s$ (~4–12) that covary positively with DOP. Although the *falciferum* Zone shales are considered to represent fully anoxic conditions (McArthur et al., 2008), TOC values are only moderate (~2–5%) and the pattern of $[Mo/TOC]_s$-DOP covariation is similar to that seen in Saanich Inlet (Fig. 10C). As at Saanich Inlet, this pattern may record redox fluctuations between oxic–suboxic and anoxic conditions at geologically short (sub-sample) timescales, yielding an organic-rich deposit whose trace-metal composition shows varying degrees of oxidative influence.

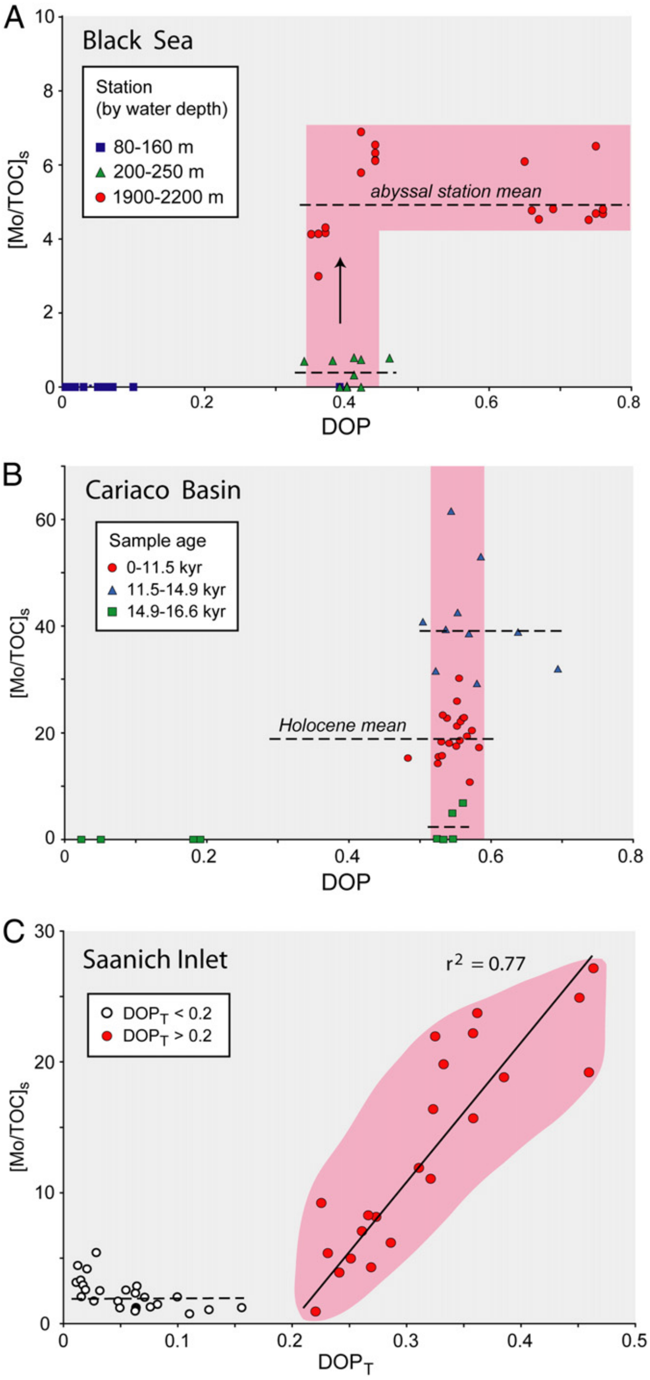

Fig. 10. $[Mo/TOC]_s$ versus DOP for modern anoxic marine systems: (A) Black Sea, (B) Cariaco Basin, and (C) Saanich Inlet. Dashed lines in A and B show average $[Mo/TOC]_s$ values for sample subsets represented by different symbols; solid line in C shows regression relationship for samples having $DOP_T > 0.2$. Black Sea DOP data from Lyons and Berner (1992) and Mo/TOC data from Algeo and Lyons (2006); all samples represent Unit I (0–1320 yr B.P.; Arthur et al., 1994). Cariaco Basin DOP and Mo/TOC data from Lyons et al. (2003); sample ages from Peterson et al. (1999). Saanich Inlet DOP_T and Mo/TOC data from François (1987); all samples <~300 yr B.P.

Although potentially indicative of a direct redox control on trace-metal accumulation, covariant relationships between $[Mo/TOC]_s$ and DOP can be produced also through indirect redox influences or incidental correlations. The latter situation may be exemplified by the Muncie Creek Shale, an Upper Pennsylvanian cyclothemic core shale from midcontinent North America (Algeo et al., 2008a). This unit exhibits significant positive covariation between DOP (over the range 0.4–0.75) and $[Mo/TOC]_s$ (Fig. 11C), which is suggestive of redox control of trace-metal accumulation. However, when examined at a finer scale (i.e., individual dm-thick cycles; cf. Algeo and Heckel, 2008, their Fig. 6), one observes that

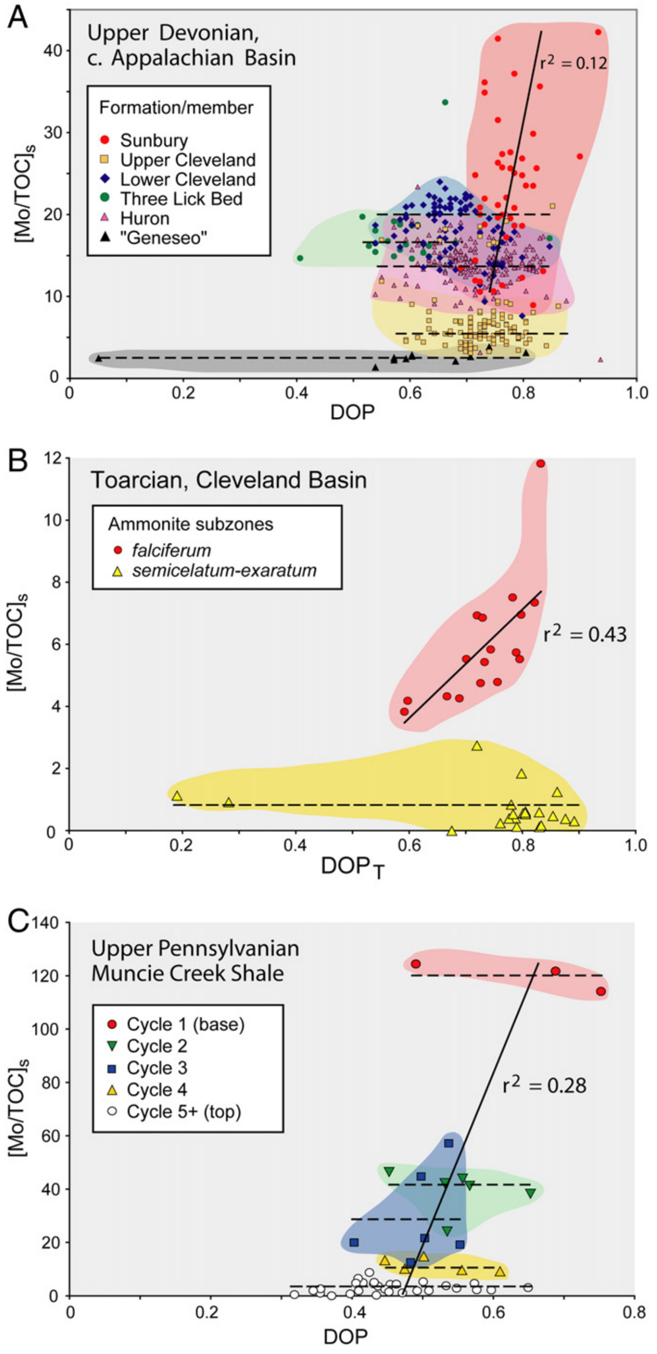

Fig. 11. $[Mo/TOC]_s$ versus DOP for paleomarine systems: (A) Upper Devonian shales, central Appalachian Basin, (B) Toarcian shales (Lower Jurassic, England), and (C) Muncie Creek Shale (Upper Pennsylvanian, Kansas). Dashed lines in A–C show average $[Mo/TOC]_s$ values for sample subsets represented by different symbols; solid lines show regression relationships for the Sunbury Shale in A, for the *falciferum* zone in B, and for the Muncie Creek Shale as a whole in C. Devonian shale data from T. Robl (unpubl.); Toarcian shale data from McArthur et al. (2008); Muncie Creek data from T. Algeo (unpubl.).

Mo/TOC ratios are fairly uniform within each cycle. This pattern is indicative of a dominant hydrographic control in which deepwater $[Mo]_{aq}$ declined progressively from one cycle to the next. Unlike for the Cariaco Basin (Fig. 10B), declining $[Mo]_{aq}$ in the Muncie Creek Shale is unlikely to be due to drawdown through removal of trace metals to the sediment, because the Late Pennsylvanian Midcontinent Sea is inferred to have had unrestricted deepwater circulation (Algeo and Maynard, 2008). Rather, this decline is more likely to reflect a progressive reduction in deepwater salinities as a result of shallowing and increased mixing with low-salinity surface waters during the regressive stage of cyclothem sedimentation (cf. Algeo and Heckel, 2008). Thus, examination of patterns of covariation between trace-metal/TOC ratios and a redox proxy such as DOP can assist in determining the relative importance of hydrographic versus redox influences on trace-metal accumulation.

5. Conclusions

An improved understanding of controls on the accumulation of trace metals in marine sediments allows new applications to paleoceanographic studies. In general, trace-metal accumulation is controlled by redox conditions in marine systems in which oxic or suboxic conditions prevail, and by hydrographic factors in marine systems that are dominantly anoxic. In the latter case, trace-metal data may allow assessment of paleoceanographic features that were previously difficult to reconstruct, such as aqueous concentrations of trace metals, the renewal time of the deep (subpycnoclinal) watermass, and short-term and long-term changes in the trace-metal inventories of seawater. Careful evaluation of trace-metal enrichment patterns in relation to redox proxies such as degree-of-pyritization (DOP) can help to confirm whether redox or hydrographic influences prevailed in a given paleomarine system.

Acknowledgments

Thanks to Tim Lyons, Barry Maynard, John McArthur, Nicolas Tribovillard, and Steven Turgeon for insightful discussions and to Thomas Robl for unpublished Devonian shale data. Research by TJA was supported by grants from the National Science Foundation (EAR-0618003, EAR-0745574, and EAR-1053449) and the University of Cincinnati Research Council.

References

Algeo, T.J., 2004. Can marine anoxic events draw down the trace-element inventory of seawater? Geology 32, 1057–1060.
Algeo, T.J., Heckel, P.H., 2008. The Late Pennsylvanian Midcontinent Sea of North America: a review. Palaeogeography Palaeoclimatology Palaeoecology 268, 205–221.
Algeo, T.J., Lyons, T.W., 2006. Mo-total organic carbon covariation in modern anoxic marine environments: implications for analysis of paleoredox and paleohydrographic conditions. Paleoceanography 21, PA1016 23 pp.
Algeo, T.J., Maynard, J.B., 2004. Trace element behavior and redox facies in core shales of Upper Pennsylvanian Kansas-type cyclothems. Chemical Geology 206, 289–318.
Algeo, T.J., Maynard, J.B., 2008. Trace metal covariation as a guide to water-mass conditions in ancient anoxic marine environments. Geosphere 4 (5), 872–887.
Algeo, T.J., Lyons, T.W., Blakey, R.C., Over, D.J., 2007. Hydrographic conditions of the Devono-Carboniferous North American Seaway inferred from sedimentary Mo–TOC relationships. Palaeogeography Palaeoclimatology Palaeoecology 256, 204–230.
Algeo, T.J., Heckel, P.H., Maynard, J.B., Blakey, R., Rowe, H., 2008a. Modern and ancient epicratonic seas and the superestuarine circulation model of marine anoxia. In: Holmden, C., Pratt, B.R. (Eds.), Dynamics of Epeiric Seas: Sedimentological, Paleontological and Geochemical Perspectives: Geological Association of Canada. Special Publication, 48, pp. 7–38.
Algeo, T.J., Rowe, H., Hower, J.C., Schwark, L., Hermann, A., Heckel, P.H., 2008b. Oceanic denitrification during Late Carboniferous glacial–interglacial cycles. Nature Geoscience 1, 709–714.
Anbar, A.D., 2004. Molybdenum stable isotopes: observations, interpretations and directions. In: Johnson, C., et al. (Ed.), Geochemistry of Non-traditional Stable Isotopes: Reviews in Mineralogy and Geochemistry, 55, pp. 429–454.
Anbar, A.D., Knoll, A.H., 2002. Proterozoic ocean chemistry and evolution; a bioinorganic bridge? Science 297, 1137–1142.
Anbar, A.D., Rouxel, O., 2007. Metal stable isotopes in paleoceanography. Annual Review of Earth and Planetary Sciences 35, 717–746.
Anbar, A.D., Duan, Y., Lyons, T.W., Arnold, G.L., Kendall, B., Creaser, R.A., Kaufman, A.J., Gordon, G.W., Scott, C., Garvin, J., Buick, R., 2007. A whiff of oxygen before the Great Oxidation Event? Science 317, 1903–1906.
Arthur, M.A., Dean, W.E., Neff, E.D., Hay, B.J., King, J., Jones, G., 1994. Varve-calibrated records of carbonate and organic carbon accumulation over the last 2000 years in the Black Sea. Global Biogeochemical Cycles 8, 195–217.
Bekker, A., Holland, H.D., Wang, P.L., Rumble, D., Stein, H.J., Hannah, J.L., Coetzee, L.L., Beukes, N.J., 2004. Dating the rise of atmospheric oxygen. Nature 427, 117–120.
Brennecka, G.A., Herrmann, A.D., Algeo, T.J., Anbar, A.D., in press. Rapid expansion of oceanic anoxia immediately before the end-Permian mass extinction. Proc. Nat. Acad. Sci. (USA).

Brezinski, D.K., Cecil, C.B., Skema, V.W., Stamm, R., 2008. Late Devonian glacial deposits from the eastern United States signal an end of the mid-Paleozoic warm period. Palaeogeography Palaeoclimatology Palaeoecology 268, 143–151.

Brumsack, H.-J., 1980. Geochemistry of Cretaceous black shales from the Atlantic Ocean (DSDP Legs 11, 14, 36 and 41). Chemical Geology 31, 1–25.

Brumsack, H.J., 2006. The trace metal content of recent organic carbon-rich sediments: implications for Cretaceous black shale formation. Palaeogeography Palaeoclimatology Palaeoecology 232, 344–361.

Canfield, D.E., 1998. A new model for Proterozoic ocean chemistry. Nature 396, 450–453.

Canfield, D.E., 2005. The early history of atmospheric oxygen. Annual Review of Earth and Planetary Sciences 33, 1–36. doi:10.1146/annurev.earth.33.092203.122711.

Chaillou, G., Schäfer, J., Blanc, G., Anschutz, P., 2008. Mobility of Mo, U, As, and Sb within modern turbidites. Marine Geology 254, 171–179.

Cohen, A.S., Coe, A.L., Harding, S.M., Schwark, L., 2004. Osmium isotope evidence for the regulation of atmospheric CO_2 by continental weathering. Geology 32, 157–160.

Dean, W.E., Piper, D.Z., Peterson, L.C., 1999. Molybdenum accumulation in Cariaco Basin sediment over the last 24 ky: a record of water-column anoxia and climate. Geology 27, 507–510.

Deuser, W.G., 1973. Cariaco Trench—oxidation of organic matter and residence time of anoxic water. Nature 242, 601–603.

Dyrssen, D.W., Hall, P.O.J., Haraldsson, C., Chierici, M., Skei, J., Östlund, H.G., 1996. Time dependence of organic matter decay and mixing processes in Framvaren, a permanently anoxic fjord in south Norway. Aquatic Geochemistry 2, 111–129.

Falkner, K.K., O'Neill, D.J., Todd, J.F., Moore, W.S., Edmond, J.M., 1991. Depletion of barium and radium-226 in Black Sea surface waters over the past thirty years. Nature 350, 491–494.

François, R., 1987. Some aspects of the geochemistry of sulphur and iodine in marine humic substances and transition metal enrichment in anoxic sediments. Ph.D. dissertation, University of British Columbia, Vancouver, B.C., Canada, 462 pp.

Glass, J.B., Wolfe-Simon, F., Anbar, A.D., 2009. Coevolution of metal availability and nitrogen assimilation in cyanobacteria and algae. Geobiology 7, 100–123.

Hardie, L.A., 1996. Secular variation in seawater chemistry: an explanation for the coupled secular variation in the mineralogies of marine limestones and potash evaporites over the past 600 m.y. Geology 24, 279–283.

Haug, G.H., Pedersen, T.F., Sigman, D.M., Calvert, S.E., Nielsen, B., Peterson, L.C., 1998. Glacial/interglacial variations in production and nitrogen fixation in the Cariaco Basin during the last 580 kyr. Paleoceanography 13, 427–432.

Hay, W.W., Migdisov, A., Balukhovsky, A.N., Wold, C.N., Flögel, S., Söding, E., 2006. Evaporites and the salinity of the ocean during the Phanerozoic: implications for climate, ocean circulation and life. Palaeogeography Palaeoclimatology Palaeoecology 240, 3–46.

Helz, G.R., Miller, C.V., Charnock, J.M., Mosselmans, J.F.W., Pattrick, R.A.D., Garner, C.D., Vaughan, D.J., 1996. Mechanism of molybdenum removal from the sea and its concentration in black shales: EXAFS evidence. Geochimica et Cosmochimica Acta 60, 3631–3642.

Helz, G.R., Bura-Nakić, E., Mikac, N., Ciglenečki, I., 2011. New model for molybdenum behavior in euxinic waters. Chemical Geology 284, 323–332.

Herrmann, A., Kendall, B., Gordon, G.W., Wasylenski, L., Algeo, T.J., Anbar, A.D., 2012-this volume. Use of molybdenum isotope data to infer paleoceanographic conditions in the Late Pennsylvanian Midcontinent Sea of North America. Chem. Geol.

Hetzel, A., Böttcher, M.E., Wortmann, U.G., Brumsack, H.-J., 2009. Paleo-redox conditions during OAE 2 reflected in Demerara Rise sediment geochemistry (ODP Leg 207). Palaeogeography Palaeoclimatology Palaeoecology 273, 302–328.

Holland, H.D., 1984. The Chemical Evolution of the Atmosphere and Oceans. Princeton University Press, Princeton, New Jersey. 582 pp.

Holmen, K.J., Rooth, C.G.H., 1990. Ventilation of the Cariaco Trench, a case of multiple source competition? Deep-Sea Research (A) 37, 203–225.

Isaacson, P.E., Díaz-Martínez, E., Grader, G.W., Kalvoda, J., Babek, O., Devuyst, F.X., 2008. Late Devonian–earliest Mississippian glaciation in Gondwanaland and its biogeographic consequences. Palaeogeography Palaeoclimatology Palaeoecology 268, 126–142.

Jenkyns, H.C., 2010. Geochemistry of oceanic anoxic events. Geochemistry Geophysics Geosystems 11 (3), Q03004 30 pp.

Johnson, J.G., Klapper, G., Sandberg, C.A., 1985. Devonian eustatic fluctuations in Euramerica. Geological Society of America Bulletin 96, 567–587.

Jones, G.A., Gagnon, A.R., 1994. Radiocarbon chronology of Black Sea sediments. Deep-Sea Research (A) 41, 531–557.

Kendall, B., Creaser, R.A., Gordon, G.W., Anbar, A.D., 2009. Re–Os and Mo isotope systematics of black shales from the Middle Proterozoic Velkerri and Wollogorang Formations, McArthur Basin, northern Australia. Geochimica et Cosmochimica Acta 73, 2534–2558.

Kendall, B., Reinhard, C.T., Lyons, T.W., Kaufman, A.J., Poulton, S.W., Anbar, A.D., 2010. Pervasive oxygenation along late Archaean ocean margins. Nature Geoscience 3, 647–652.

Kieffer, F., 1991. Metals as essential trace elements for plants, animals, and humans. In: Merian, E. (Ed.), Metals and Their Compounds in the Environment. Wiley-VCH, Weinheim, Germany, pp. 481–489.

Lee, B.-S., Bullister, J.L., Murray, J.W., Sonnerup, R.E., 2002. Anthropogenic chlorofluorocarbons in the Black Sea and the Sea of Marmara. Deep-Sea Research (I) 49, 895–913.

Logan, G.A., Hayes, J.M., Hieshima, G.B., Summons, R.E., 1995. Terminal Proterozoic reorganization of biogeochemical cycles. Nature 376, 53–56.

Loucks, R.G., Ruppel, S.C., 2007. Mississippian Barnett Shale: lithofacies and depositional setting of a deep-water shale-gas succession in the Fort Worth Basin. Texas American Association of Petroleum Geologists Bulletin 91, 579–601.

Lowenstein, T.K., Demicco, R.V., Hardie, L.A., Timofeeff, M.N., 2003. Secular variation in seawater chemistry and the origin of calcium chloride basinal brines. Geology 31, 857–860.

Lyons, T.W., 1991. Upper Holocene sediments of the Black Sea: summary of Leg 4 box cores (1988 Black Sea Oceanographic Expedition). In: Izdar, E., Murray, J.W. (Eds.), Black Sea Oceanography. Springer, New York, pp. 401–441.

Lyons, T.W., Berner, R.A., 1992. Carbon–sulfur–iron systematics of the uppermost deep-water sediments of the Black Sea. Chemical Geology 99, 1–27.

Lyons, T.W., Werne, J.P., Hollander, D.J., Murray, R.W., 2003. Contrasting sulfur geochemistry and Fe/Al and Mo/Al ratios across the last oxic-to-anoxic transition in the Cariaco Basin, Venezuela. Chemical Geology 195, 131–157.

Lyons, T.W., Anbar, A.D., Severmann, S., Scott, C., Gill, B.C., 2009. Tracking euxinia in the ancient ocean: a multiproxy perspective and Proterozoic case study. Annual Review of Earth and Planetary Sciences 37, 507–534.

März, C., Beckmann, B., Franke, C., Vogt, C., Wagner, T., Kasten, S., 2009. Geochemical environment of the Coniacian–Santonian western tropical Atlantic at Demerara Rise. Palaeogeography Palaeoclimatology Palaeoecology 273, 286–301.

McArthur, J.M., Howarth, R.J., Bailey, T.R., 2001. Strontium isotope stratigraphy: LOWESS version 3: best fit to the marine Sr-isotope curve for 0–509 Ma and accompanying look-up table for deriving numerical age. Journal of Geology 109, 155–170.

McArthur, J.M., Algeo, T.J., van de Schootbrugge, B., Li, Q., Howarth, R.J., 2008. Basinal restriction, black shales, and the Early Toarcian (Jurassic) oceanic anoxic event. Paleoceanography 23, PA4217. doi:10.1029/2008PA001607.

McManus, J., Berelson, W.M., Severmann, S., Poulson, R.L., Hammond, D.E., Klinkhammer, G.P., Holm, C., 2006. Molybdenum and uranium geochemistry in continental margin sediments: paleoproxy potential. Geochimica et Cosmochimica Acta 70, 4643–4662.

Montoya-Pino, C., Weyer, S., Anbar, A.D., Pross, J., Oschmann, W., van de Schootbrugge, B., Arz, H.W., 2010. Global enhancement of ocean anoxia during Oceanic Anoxic Event 2: a quantitative approach using U isotopes. Geology 38, 315–318.

Murray, J.W., Top, Z., Oszoy, E., 1991. Hydrographic properties and ventilation of the Black Sea. Deep-Sea Research (A) 38, S663–S689.

Östlund, H.G., Dyrssen, D., 1986. Renewal rates of the Black Sea deep water. The Chemical and Physical Oceanography of the Black Sea, Reports of the Chemistry of the Sea XXXIII. University of Göteborg, Göteborg, Sweden.

Pashin, J.C., Ettensohn, F.R., 1995. Reevaluation of the Bedford–Berea sequence in Ohio and adjacent states: forced regression in a foreland basin. Geological Society of America Special Paper, 298. 68 pp.

Pattan, J.N., Pearce, N.J.G., 2009. Bottom water oxygenation history in southeastern Arabian Sea during the past 140 ka: results from redox-sensitive elements. Palaeogeography Palaeoclimatology Palaeoecology 280, 396–405.

Pearce, C.R., Cohen, A.S., Coe, A.L., Burton, K.W., 2008. Molybdenum isotope evidence for global ocean anoxia coupled with perturbations to the carbon cycle during the Early Jurassic. Geology 36, 231–234.

Pegram, W., Turekian, K., 1999. The osmium isotope composition change of Cenozoic sea water inferred from a deep-sea core corrected for meteoritic contributions. Geochimica et Cosmochimica Acta 63, 4053–4058.

Peterson, L.C., Haug, G.H., Murray, R.W., Yarincik, K.M., King, J.W., Bralower, T.J., Kameo, K., Pearce, R.B., 1999. Late Quaternary stratigraphy and sedimentation at ODP Site 1002, Cariaco Basin (Venezuela). Proceedings of the Ocean Drilling Program Science Research 165, 85–99.

Playford, P.E., Hurley, N.F., Kerans, G., Middleton, M., 1989. Reefal platform development, Devonian of the Canning Basin, Western Australia. In: Crevello, P.D., Wilson, J.L., Sarg, J.F., Read, J.F. (Eds.), Controls on Carbonate Platforms and Basin Development: Soc. Econ. Paleontol. Mineral. Spec. Publ., 44, pp. 187–202.

Raiswell, R., Buckley, F., Berner, R.A., Anderson, T.F., 1988. Degree of pyritization of iron as a paleoenvironmental indicator of bottom-water oxygenation. Journal of Sedimentary Petrology 58, 812–819.

Richards, F.A., 1975. The Cariaco Basin (Trench). Oceanography and Marine Biology Annual Reviews 13, 11–67.

Rowe, H.D., Loucks, R.G., Ruppel, S.C., Rimmer, S.M., 2008. Mississippian Barnett Formation, Fort Worth Basin, Texas: bulk geochemical inferences and Mo–TOC constraints on the severity of hydrographic restriction. Chemical Geology 257, 16–25.

Rowe, H., Ruppel, S., Rimmer, S., Loucks, R., 2009. Core-based chemostratigraphy of the Barnett Shale, Permian Basin, Texas. Gulf Coast Association of Geological Societies Transactions 59, 675–686.

Scopelliti, G., Bellanca, A., Neri, R., Baudin, F., Coccioni, R., 2006. Comparative high-resolution chemostratigraphy of the Bonarelli Level from the reference Bottaccione section (Umbria–Marche Apennines) and from an equivalent section in NW Sicily: consistent and contrasting responses to the OAE-2. Chemical Geology 228, 266–285.

Scott, C., Lyons, T.W., Bekker, A., Shen, Y., Poulton, S.W., Chu, X., Anbar, A.D., 2008. Tracing the stepwise oxygenation of the Proterozoic ocean. Nature 452, 456–459.

Scranton, M.I., Sayles, F.L., Bacon, M.P., Brewer, P.G., 1987. Temporal changes in the hydrography and chemistry of the Cariaco Trench. Deep-Sea Research (A) 34, 945–963.

Skei, J., 1983. Geochemical and sedimentological considerations of a permanently anoxic fjord—Framvaren, south Norway. Sedimentary Geology 36, 131–145.

Sloss, L.L., 1963. Sequences in the cratonic interior of North America. Geological Society of America Bulletin 74, 93–113.

Sternbeck, J., Sohlenius, G., Hallberg, R.O., 2000. Sedimentary trace elements as proxies to depositional changes induced by a Holocene fresh–brackish water transition. Aquatic Geochemistry 6, 325–345.

Strauss, H., 1999. Geological evolution from isotope proxy signals—sulfur. Chemical Geology 161, 89–101.

Suan, G., Pittet, B., Bour, Y., Mattioli, E., Duarte, L.V., Mailliot, S., 2008. Duration of the Early Toarcian carbon isotope excursion deduced from spectral analysis: consequence for its possible causes. Earth and Planetary Science Letters 267, 666–679.

Top, Z., Clarke, W.B., 1983. Helium, neon and tritium in the Black Sea. Journal of Marine Research 41, 1–17.

Top, Z., Izdar, E., Ergün, M., Konuk, T., 1990. Evidence of tectonism from ^{3}He and residence time of helium in the Black Sea. Eos (Transactions AGU) 71 (32), 1020–1021.

Tribovillard, N., Algeo, T.J., Lyons, T.W., Riboulleau, A., 2006. Trace metals as paleoredox and paleoproductivity proxies: an update. Chemical Geology 232, 12–32.

Turgeon, S., Brumsack, H.-J., 2006. Anoxic vs. dysoxic events reflected in sediment geochemistry during the Cenomanian–Turonian Boundary Event (Cretaceous) in the Umbria–Marche Basin of Italy. Chemical Geology 234, 321–339.

Tyson, R.V., Pearson, T.H., 1991. Modern and ancient continental shelf anoxia: an overview. In: Tyson, R.V., Pearson, T.H. (Eds.), Modern and Ancient Continental Shelf Anoxia: Geol. Soc. London Spec. Publ., 58, pp. 1–24.

van der Weijden, C.H., Reichart, G.-J., van Os, B.J.H., 2006. Sedimentary trace element records over the last 200 kyr from within and below the northern Arabian Sea oxygen minimum zone. Marine Geology 231, 69–88.

Veizer, J., Ala, D., Azmy, K., Bruckschen, P., Buhl, D., Bruhn, F., Carden, G.A.F., Diener, A., Ebneth, S., Godderis, Y., Jasper, T., Korte, C., Pawellek, F., Podlaha, O.G., Strauss, H., 1999. ^{87}Sr/^{86}Sr, δ^{13}C and δ^{18}O evolution of Phanerozoic seawater. Chemical Geology 161, 59–88.

Weyer, S., Anbar, A.D., Gerdes, A., Gordon, G., Algeo, T.J., Boyle, E.A., 2008. Natural fractionation of ^{238}U/^{235}U. Geochimica et Cosmochimica Acta 72, 345–359.

Wille, M., Nägler, T.F., Lehmann, B., Schröder, S., Kramers, J.D., 2008. Hydrogen sulphide release to surface waters at the Precambrian/Cambrian boundary. Nature 453, 767–769.

Wright, J., Colling, A., 1995. Seawater: Its Composition, Properties and Behaviour, 2nd ed. Elsevier, New York. 168 pp.

Xu, G., Hannah, J.L., Stein, H.J., Bingen, B., Yang, G., Zimmerman, A., Weitschat, W., Mørk, A., Weiss, H.M., 2009. Re–Os geochronology of Arctic black shales to evaluate the Anisian–Ladinian boundary and global faunal correlations. Earth and Planetary Science Letters 288, 581–587.

Yao, W., Millero, F.J., 1995. The chemistry of the anoxic waters in the Framvaren Fjord. Norway Aquatic Geochemistry 1, 53–88.

Yarincik, K.M., Murray, R.W., Lyons, T.W., Peterson, L.C., Haug, G.H., 2000. Oxygenation history of bottom waters in the Cariaco Basin, Venezuela, over the past 578,000 years: results from redox-sensitive metals (Mo, V, Mn, and Fe). Paleoceanography 15, 593–604.

Zhang, J.-Z., Millero, J.J., 1993. The chemistry of anoxic waters in the Cariaco Trench. Deep-Sea Research (I) 40, 1023–1041.

Zheng, Y., Anderson, R.F., van Geen, A., Kuwabara, J.S., 2000. Authigenic molybdenum formation in marine sediments: a linkage to pore water sulfide in the Santa Barbara Basin. Geochimica et Cosmochimica Acta 64, 4165–4178.